Wetting Transition in Water

S. R. Friedman, M. Khalil, and P. Taborek

Department of Physics and Astronomy, University of California, Irvine, Irvine, California 92697, USA

(Received 10 September 2013; published 26 November 2013)

Optical images were used to study the wetting behavior of water on graphite, sapphire, and quartz along the liquid vapor coexistence curve from room temperature to 300 °C. Wetting transitions were identified by the temperature at which the contact angle decreased to zero and also by the disappearance of dropwise condensation. These two methods yielded consistent values for the wetting temperatures, which were 185 °C, 234 °C, and 271 °C for water on quartz, sapphire, and graphite, respectively. We compare our results with the theoretical predictions based on a simplified model of the water-substrate potential and sharp interfaces.

DOI: 10.1103/PhysRevLett.111.226101 PACS numbers: 68.08.Bc, 68.35.Rh

A drop of fluid placed on a solid substrate will spread until it reaches a minimum energy configuration. Qualitatively, the form of the minimum energy configuration is determined by the ratio of the potential energy of interaction between two fluid molecules and a fluid molecule and the substrate. If the fluid interacts strongly with itself, the minimum energy configuration will be a compact shape with a finite contact angle, while if the opposite is true, the fluid will spread into a thin pancake film with essentially zero contact angle. The Young equation, $\sigma_{vs}(T) = \sigma_{ls}(T) + \sigma_{lv}(T)\cos[\theta(T)]$ is the quantitative expression of this balance expressed in terms of the contact angle θ and the energetic cost per unit area at temperature T of the liquid-solid, liquid-vapor, and vapor-solid interfaces denoted by $\sigma_{ls}(T)$, $\sigma_{lv}(T)$, and $\sigma_{vs}(T)$, respectively. The wetting properties of the liquid are characterized by the value of the contact angle θ: if $\theta(T) > 0$, a liquid drop forms on the solid surface and the liquid is said to partially wet the solid, while if $\theta = 0$ the liquid completely wets the solid and forms a film on a surface.

The wetting properties depend on temperature through the temperature dependence of the surface energies. In particular, the liquid-vapor surface tension $\sigma_{lv}(T)$ is nonnegative and represents a cost of spreading, but it approaches zero at the bulk liquid-vapor critical temperature T_c because the phases become indistinguishable. Cahn [1] showed that even if a liquid did not completely wet a surface at a certain temperature, then in general either the liquid or the vapor will completely wet the surface at some characteristic temperature called the wetting temperature T_w, with $T_w < T_c$. This transition from partial wetting to complete wetting is called the wetting transition and is a first-order phase transition [2,3].

Despite the generality of the wetting transition scenario, it has been experimentally observed in only a few systems, including cryogenic fluids [4–11], room temperature binary liquid mixtures [2,3,12], and liquid mercury [13,14]. In order to predict the wetting temperature, the values of the interfacial energies and their temperature dependence must be calculated, which is a delicate and challenging task. A simplified model developed for the cryogenic liquids [15,16] treats the solid-liquid interface as equivalent to a bulklike liquid vapor interface, a vapor-solid interface, and the work of adhesion between the two interfaces which can be expressed as an integral of the interaction potential $V(z)$ between a molecule in the fluid and the semi-infinite solid. This approximation eliminates σ_{vs} and σ_{ls} from the problem, and the contact angle can be expressed in terms of $\sigma_{lv}(T)$ as

$$\cos[\theta(T)] = -1 - \frac{\Delta\rho(T)}{\sigma_{lv}(T)} \int_{z_{min}}^{\infty} V(z)dz, \tag{1}$$

where $\Delta\rho$ is the difference between the liquid and vapor densities. The temperature dependence of the contact angle comes from the temperature dependence of $\Delta\rho$ and σ_{lv}, both of which are experimentally measurable. The potential can be parametrized using the Lennard-Jones 3–9 potential

$$V(z) = \frac{4C_3^3}{27D^2z^9} - \frac{C_3}{z^3}, \tag{2}$$

where C_3 is the van der Waals coefficient, D is the well depth, and $z_{min} = (2C_3/3D)^{1/3}$. For this simple form of potential, the integral in Eq. (1) can be done exactly; the result depends on a single parameter C_3D^2, and any choice of this parameter determines the behavior of the contact angle as a function of temperature. The wetting temperature is determined by the solution to the equation

$$3.33\frac{\Delta\rho(T_w)}{\sigma_{lv}(T_w)} = (C_3D^2)^{1/3}. \tag{3}$$

An alternative way to parametrize the solutions to Eq. (1) which emphasizes experimentally determined quantities is to use the value of the contact angle at any convenient fixed temperature T_0. $\theta(T_0)$ determines C_3D^2 and establishes a relationship between $\theta(T_0)$ and T_w which is independent of

the substrate. A plot of this relationship for water with $T_0 = 30\,^{\circ}\mathrm{C}$ is shown in Fig. 1.

This simplified model has proven to be quite reliable for fluids such as helium and hydrogen on weakly interacting substrates [17,18]. Water, however, is significantly different from the cryogenic fluids because it is polar and hydrogen bonds make up a significant fraction of the cohesive energy. Adsorption isotherms [19–21] and direct force measurements [22–24] in water yield results that cannot be explained using van der Waals forces alone. For water, additional terms that describe electrostatic effects and a ''structural force'' due to spatial gradients in the hydrogen bond network near the interface must be included, which adds terms proportional to Az^{-2} and $Ke^{-z/\lambda}$ to Eqs. (1) and (2) [25,26]. The values of the parameters A, K, and λ and their temperature dependence are not well established and are difficult to relate to first principles theory.

Somewhat counterintuitively, pure water does not wet most solid substrates at room temperature. The general thermodynamic argument described above implies that water should wet these substrates at sufficiently high temperatures, but to our knowledge, the wetting temperature of water has has not been experimentally determined for any substrate. The temperature dependence of the contact angle and the wetting temperature provide important constraints on the models of the interaction potential and the fluid interface. We chose quartz, sapphire, and graphite for our experimental substrates because of their chemical compatibility with high temperature water and because they span a wide range of interaction strengths with water, as measured by the room temperature contact angles.

Our experimental apparatus consisted of a gold plated stainless steel cell with a volume of approximately 35 cm^3. The cell had two coaxial sapphire windows (5 cm diam, 1.5 cm thick) which were sealed to the cell using die-molded graphite o rings. The cell was filled approximately

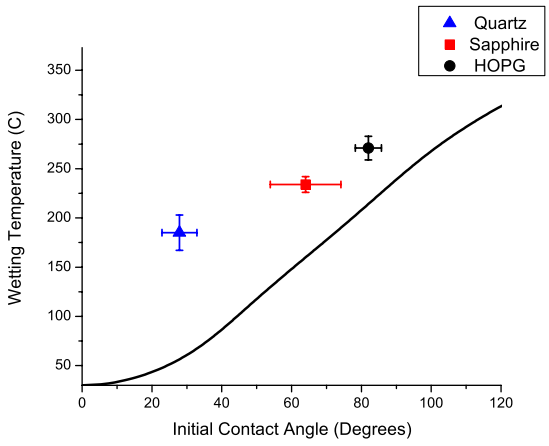

FIG. 1 (color online). Universal plot of the wetting temperature of water on any substrate as a function of the initial contact angle at 30 °C. Symbols show experimental values for HOPG, sapphire, and quartz.

half full of millipore filtered DI water at room temperature and then sealed using a conflat fitting with a gold plated copper gasket. In some experiments, the water was degassed by boiling *in situ*, but this did not seem to noticeably affect the results. Because the cell was sealed at room temperature, the pressure in the cell was determined by the vapor pressure of water at the cell temperature. The solid substrates under investigation were positioned in the middle of the windows using graphite supports. Sapphire and quartz substrates were cleaned using isopropyl alcohol, while HOPG substrates were prepared by cleaving a fresh surface prior to every run.

Several precautions were taken to minimize temperature gradients in the cell. The cell was equipped with a thermocouple and a platinum thermometer, but was heated indirectly through radiation. The cell was mounted inside an oven on macor supports. The oven containing the cell was mounted inside a vacuum can and surrounded by three independent highly reflective aluminum radiation shields with apertures containing IR reflecting hot mirrors aligned along the axis of the cell windows. The total power required to keep the cell at 300 °C was approximately 50 W. The distance from the center of the cell to the outside vacuum can windows was approximately 30 cm. A computer controlled DSLR camera with a long distance microscope lens was used to take images of the experiment.

We used two substrate configurations to locate the wetting transition temperature. In the first configuration, the substrate was mounted vertically with half of its surface submerged under liquid and half exposed to water vapor. In the second configuration, the substrate surface was mounted horizontally with the top surface exposed to vapor. A liquid drop was placed on the substrate at room temperature before the cell was sealed. In both cases, the temperature of the cell was increased from room temperature to the final temperature at a rate in the range of 7–15 deg/h.

In the first type of experiment, the characteristic feature of the wetting transition was a transition from dropwise to filmwise condensation. For this ''condensation experiment'', the substrate was frontlit in the case of opaque materials and backlit in the case of transparent materials. Images were taken at regular intervals of 300 sec as the temperature of the system was ramped to the desired ending point. Despite our precautions, the finite heating rate and the symmetric position of the cell in the oven implies that the center of the cell where the vertical substrate was mounted was slightly cooler than the outside surfaces of the cell. This temperature difference, which we estimate to be approximately 1°, caused condensation on the exposed vertical surface. Below the wetting temperature, the condensation formed droplets with finite contact angles and significant curvature which made them easily visible. Droplets would grow, merge, and drain away and were replaced by new droplets which grew from the vapor.

At high temperatures, the wetted interface was flat and smooth with no droplets visible. Because droplets with small contact angle become difficult to see, the wetting temperature could be determined to within $\pm 5\,^{\circ}\mathrm{C}$. Figure 2 shows an example of images of the condensation experiment using graphite. See the Supplemental Material [27] for the time lapse video that shows the evolution of this transition. Similar images were obtained for all of the substrates investigated.

The condensation experiments provide a robust method of measuring the wetting temperature. In the simple model of Eq. (1), the wetting temperature determines the relevant combination of parameters in the potential which in turn generates a prediction for the temperature dependence of the contact angle. To check this prediction, a second type of experiment was required. This second experiment utilized images of a sessile drop as a function of temperature to measure the contact angle as shown in Fig. 3; the wetting temperature is identified as the temperature at which the contact angle goes to zero.

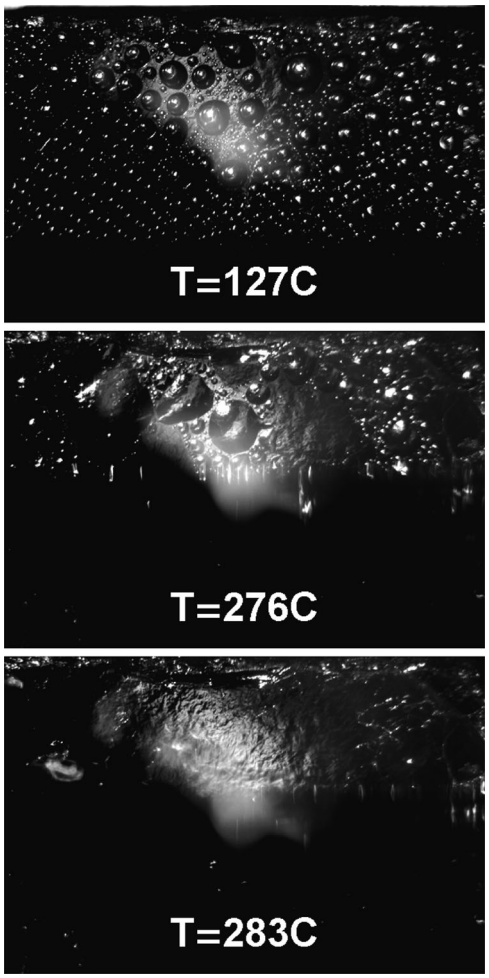

FIG. 2. Condensation measurement using graphite. The images show a front lit vertical graphite plate. The upper portion is in contact with vapor while the lower portion (which appears black) is submerged under liquid. In the upper two panels, drop condensation is clearly visible. In the lower panel, a smooth thin film has formed. See Supplemental Material [27] for video which shows the transition from non-wetting to wetting.

Images for the "contact angle experiment" were taken in a similar manner as the "condensation experiment." The drop was backlit in order to produce a high contrast image of the drop profile. The initial drop volume was typically 30 μl, which generated gravitationally flattened drops; smaller drops closer to a spherical cap shape tended to evaporate before the end of the experiment. The drop shape was extracted from each image using a Sobel filter for edge detection in Mathematica.

In principle, the contact angle can be determined by examining the drop shape near the contact line, but in practice optical artifacts in the image near the substrate as well as condensation on the surface of the substrate made the baseline unclear. Instead, we did a global fit of the entire profile to solutions of the Young-Laplace equation [$\Delta\rho g h = \sigma_{\mathrm{lv}}(1/R_1 + 1/R_2)$], where R_1 and R_2 are the principal radii of curvature and h is the height above the substrate. For an axisymmetric drop, this yields a single nonlinear ODE which can be solved for suitable boundary conditions as described in the Supplemental Material [27].

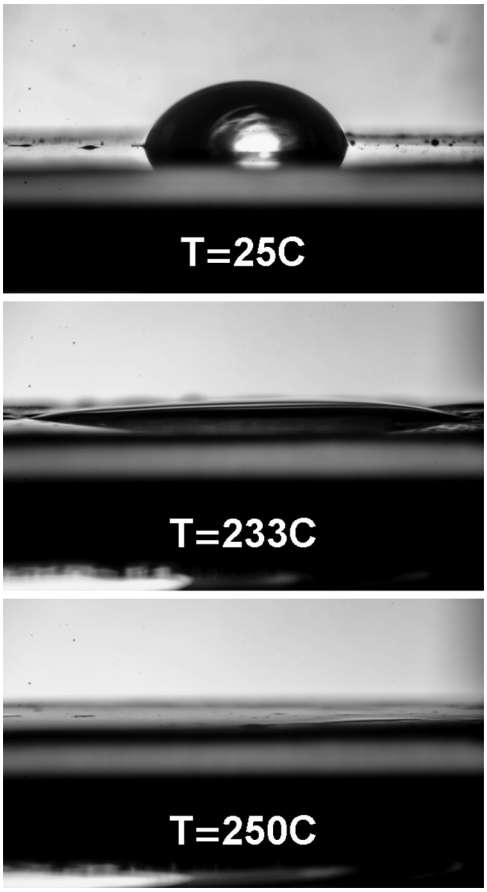

FIG. 3. Series of images showing the progression of the contact angle of water on sapphire. The bottom image shows the system after the wetting transition has already occurred.

The contact angle and drop volume for each drop were obtained from the best fit. Values for the surface tension and density difference was taken from NIST tables [28,29]. Images were obtained every few degrees until the contact angle became unmeasurably small, usually at around 5°. Measurements were performed for a range of initial drop sizes. The fitting procedure yielded a contact angle with less than 1° of uncertainty, but contact line pinning and stick-slip motion introduced variations from drop to drop of up to 13°. For this reason, the data shown in Fig. 4 are an average of contact angles measured for at least 5 different drops. The contact angle measurements and the condensation measurements are complementary. The contact angle measurements rely on measurements of a single drop which can be affected by contact line pinning and are difficult to resolve at low contact angle, but they provide information over a wide range of temperatures. The condensation measurements utilize growing drops with advancing contact lines which can be used to locate the wetting temperature, but this type of measurement is not useful for determining the behavior of the contact angle at lower temperatures.

Our measurements on sapphire were motivated by the need to understand the wetting behavior of our experimental cell windows. The sapphire substrate was a C axis crystal with a scratch-dig of 10–5. The contact angle of water on the sapphire substrate at room temperature was 64° ± 10° at 30 °C. The average of a series of contact angle measurements is shown in Fig. 4. The averaged results from both the contact angle and condensation experiments were consistent within error and yielded an average wetting temperature of 234 °C ± 8 °C for water on sapphire. The quartz substrates we used were 2.5 cm square Z cut quartz plates polished on both sides. The contact angle at room temperature is 28° ± 5°. The temperature dependence of the contact angle is shown in Fig. 4.

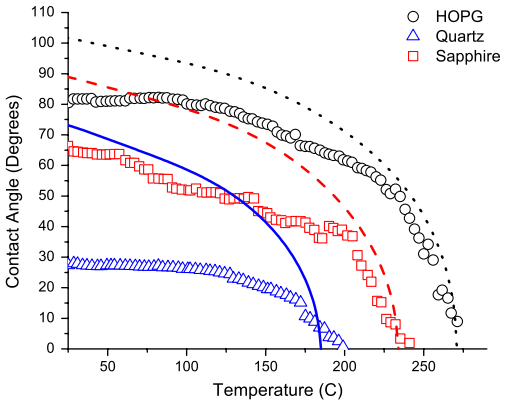

FIG. 4 (color online). Experimental measurements of the contact angle as a function of temperature of water on quartz, sapphire, and graphite. The curves are the function defined by Eq. (1) with the parameter C_3D^2 adjusted to match the observed wetting temperature.

The averaged wetting temperature from both experiments for quartz was approximately 185 °C ± 18 °C.

Figure 4 also shows the dependence of the contact angle as a function of temperature for water on highly ordered pyrolytic graphite (HOPG). The contact angle of water on HOPG is 82° ± 10° at 30 °C. The contact angle and condensation experimental data were, once again, consistent within error and yielded a wetting temperature of approximately 271 ± 12 °C, where the vapor pressure is approximately 60 atm. In contrast to sapphire and quartz, the graphite-water interaction has been extensively studied using a variety of theoretical techniques [30–35]. Recent numerical simulations predict values of the wetting temperature of 197 °C ± 5 °C [35] and 203 °C ± 5 °C [34]. Predictions from the sharp-kink approximation find a wetting transition in the range 75 °C–225 °C, which depends rather sensitively on the assumed form of the potential [32]. Figure 4 shows curves for the simplified theory with parameter values chosen to match the average observed wetting temperature. The values obtained are $(C_3D^2)^{1/3} = 180$, 230, and 291 meV Å, respectively for HOPG, sapphire, and quartz. With this constraint, the model tends to overestimate the room temperature values of the contact angle. For example, the contact angle at room temperature using the sharp-kink approximation solution from Gatica *et al.* [32] is approximately 97° at 25 °C, while the measured value is approximately 82°. Similarly, Fig. 1 shows that for a given room temperature contact angle, the simplified model systematically underestimates the wetting temperature.

Wetting transitions are known to be extremely thermally hysteretic; i.e., a wetting film can be cooled far below the wetting temperature into a metastable state which can be very long lived due to the high energetic cost of nucleating a dry spot [4,36–39]. Thermal hysteresis measurements in the contact angle experiment were not feasible because of the complications of contact angle hysteresis and because we could not introduce a new drop to form an advancing contact line in our current apparatus. In the case of the condensation-type of experiments, when the cell was cooled, the direction of the heat flux was reversed and the condensation formed on the cell windows rather than on the substrate in the center. In the case of sapphire, we could exploit this effect to confirm strong thermal hysteresis in the wetting behavior: if the cell was heated to slightly below the wetting temperature and then cooled, condensation droplets formed on the window, but if the cell was heated to slightly above the wetting temperature and then cooled, no condensation drops were visible.

In conclusion, we measured the contact angle of water as a function of temperature for sapphire, quartz, and graphite and found the wetting transition temperatures; these temperatures coincide with the temperatures at which we observe a transition between dropwise and filmwise condensation. The wetting temperature on the various

substrates increases monotonically with the contact angle at room temperature. Our experimentally observed value of the wetting temperature on graphite is slightly higher than all of the recent model predictions. The sharp-kink approximation is qualitatively consistent with our data, but it does not seem possible to simultaneously account for the observed values of the wetting temperature and the room temperature contact angle using a van der Waals type of potential. The discrepancy between these two values systematically increases as the initial contact angle decreases.

This work was supported by NSF DMR-0907495.

[1] J. W. Cahn, J. Chem. Phys. **66**, 3667 (1977).
[2] D. Bonn and D. Ross, Rep. Prog. Phys. **64**, 1085 (2001).
[3] B. M. Law, Prog. Surf. Sci. **66**, 159 (2001).
[4] J. E. Rutledge and P. Taborek, Phys. Rev. Lett. **69**, 937 (1992).
[5] E. Cheng, G. Mistura, H. C. Lee, M. H. W. Chan, M. W. Cole, C. Carraro, W. F. Saam, and F. Toigo, Phys. Rev. Lett. **70**, 1854 (1993).
[6] J. Klier, P. Stefanyi, and A. F. G. Wyatt, Phys. Rev. Lett. **75**, 3709 (1995).
[7] D. Ross, J. E. Rutledge, and P. Taborek, Phys. Rev. Lett. **76**, 2350 (1996).
[8] G. B. Hess, M. J. Sabatini, and M. H. W. Chan, Phys. Rev. Lett. **78**, 1739 (1997).
[9] J. E. Rutledge, D. Ross, and P. Taborek, J. Low Temp. Phys. **113**, 811 (1998).
[10] D. Ross, P. Taborek, and J. E. Rutledge, J. Low Temp. Phys. **111**, 1 (1998).
[11] D. Ross, P. Taborek, and J. E. Rutledge, Phys. Rev. B **58**, R4274 (1998).
[12] H. Kellay, D. Bonn, and J. Meunier, Phys. Rev. Lett. **71**, 2607 (1993).
[13] M. Yao and F. Hensel, J. Phys. Condens. Matter **8**, 9547 (1996).
[14] V. F. Kozhevnikov, D. I. Arnold, S. P. Naurzakov, and M. E. Fisher, Phys. Rev. Lett. **78**, 1735 (1997).
[15] E. Cheng, M. W. Cole, W. F. Saam, and J. Treiner, Phys. Rev. Lett. **67**, 1007 (1991).
[16] S. M. Gatica and M. W. Cole, J. Low Temp. Phys. **157**, 111 (2009).
[17] E. Cheng, M. W. Cole, J. Dupont-Roc, W. F. Saam, and J. Treiner, Rev. Mod. Phys. **65**, 557 (1993).
[18] R. Garcia, K. Osborne, and E. Subashi, J. Phys. Chem. B **112**, 8114 (2008).
[19] V. Panella, R. Chiarello, and J. Krim, Phys. Rev. Lett. **76**, 3606 (1996).
[20] H. J. Muller, Langmuir **14**, 6789 (1998).
[21] D. Bhatt, J. Newman, and C. J. Radke, J. Phys. Chem. B **107**, 13 076 (2003).
[22] R. H. Yoon, D. H. Flinn, and Y. I. Rabinovich, J. Colloid Interface Sci. **185**, 363 (1997).
[23] E. E. Meyer, K. J. Rosenberg, and J. Israelachvili, Proc. Natl. Acad. Sci. U.S.A. **103**, 15 739 (2006).
[24] M. U. Hammer, T. H. Anderson, A. Chaimovich, M. S. Shell, and J. Israelachvili, Faraday Discuss. **146**, 299 (2010).
[25] N. V. Churaev, Adv. Colloid Interface Sci. **58**, 87 (1995).
[26] N. V. Churaev and V. D. Sobolev, Adv. Colloid Interface Sci. **61**, 1 (1995).
[27] See Supplemental Material at http://link.aps.org/supplemental/10.1103/PhysRevLett.111.226101 for a time lapse video that shows the transition from nonwetting to wetting on a graphite plate and a description of the image processing and data analysis techniques used to extract a sessile drop profile from digital images in order to compare these profiles with ones computed from the Young-Laplace equation.
[28] N. B. Vargaftik, B. N. Volkov, and L. D. Voljak, J. Phys. Chem. Ref. Data **12**, 817 (1983).
[29] W. Wagner and A. Pruss, J. Phys. Chem. Ref. Data **31**, 387 (2002).
[30] T. Werder, J. H. Walther, R. L. Jaffe, T. Halicioglu, and P. Koumoutsakos, J. Phys. Chem. B **107**, 1345 (2003).
[31] A. Pertsin and M. Grunze, J. Phys. Chem. B **108**, 1357 (2004).
[32] S. M. Gatica, J. K. Johnson, X. C. Zhao, and M. W. Cole, J. Phys. Chem. B **108**, 11 704 (2004).
[33] X. C. Zhao and J. K. Johnson, Mol. Simul. **31**, 1 (2005).
[34] X. C. Zhao, Phys. Rev. B **76**, 041402 (2007).
[35] R. C. Dutta, S. Khan, and J. K. Singh, Fluid Phase Equilib. **302**, 310 (2011).
[36] M. Schick and P. Taborek, Phys. Rev. B **46**, 7312 (1992).
[37] D. Bonn, H. Kellay, and J. Meunier, Phys. Rev. Lett. **73**, 3560 (1994).
[38] R. Bausch, R. Blossey, and M. A. Burschka, J. Phys. A **27**, 1405 (1994).
[39] D. Bonn, E. Bertrand, J. Meunier, and R. Blossey, Phys. Rev. Lett. **84**, 4661 (2000).